The 3-Hydroxy Group and 4,5-*trans* Double Bond of Sphingomyelin Are Essential for Modulation of Galactosylceramide Transmembrane Asymmetry

Barbara Malewicz,* Jacob T. Valiyaveettil,† Kochurani Jacob,† Hoe-Sup Byun,† Peter Mattjus,* Wolfgang J. Baumann,* Robert Bittman,† and Rhoderick E. Brown*

*University of Minnesota, Hormel Institute, Austin, Minnesota 55912; and †Department of Chemistry and Biochemistry, Queens College of the City University of New York, Flushing, New York 11367

ABSTRACT The structural features of SPM that control the transbilayer distribution of β-GalCer in POPC vesicles were investigated by ^{13}C- and ^{31}P-NMR spectroscopy using lipid analogs that share physical similarities with GalCer or SPM. The SPM analogs included *N*-palmitoyl-4,5-dihydro-SPM, 3-deoxy-SPM, 1-alkyl-2-amidophosphatidylcholine, and dipalmitoylphosphatidylcholine, a popular model "raft lipid". The transbilayer distributions of the SPM analogs and SPM in POPC vesicles were similar by ^{31}P-NMR. To observe the dramatic change in GalCer transbilayer distribution that occurs when SPM is included in POPC vesicles, the 3-OH group, 4,5-*trans* double bond, and amide linkage all were required in SPM. However, inclusion of 2 and 10 mol % dihydroSPM in SPM/POPC (1:1) vesicles mitigated and completely abrogated the effect of SPM on the transbilayer distribution of GalCer. Despite sharing some structural features with GalCer and localizing preferentially to the inner leaflet of POPC vesicles, dimyristoylphosphatidylethanolamine did not undergo a change in transbilayer distribution when SPM was incorporated into the vesicles. The results support the hypothesis that specific interactions may be favored among select sphingolipids in curvature-stressed membranes and emphasize the potential importance of the SPM-dihydroSPM ratio in membrane fission and fusion processes associated with vesicle biogenesis and trafficking.

INTRODUCTION

SPM is a key membrane component of higher eukaryotes. This sphingophospholipid provides a reservoir of messenger signals that mediate processes such as programmed cell death, cellular stress, mitogenesis, and senesce (Andrieu-Abadie and Levade, 2002; Bektas and Spiegel, 2004; Futerman and Hannun, 2004; Kolesnick, 2002). SPM also appears to be an important structural constituent of raft and caveolar microdomains in biomembranes (Brown, 1998; Edidin, 2003; Simons and Vaz, 2004). The putative function of rafts as organizing platforms for certain lipid-anchored proteins involved in cell signaling has been ascribed to the liquid-ordered environment existing within such microdomains (Brown and London, 2000; Rietveld and Simons, 1998; Simons and Ikonen, 1997). Accordingly, the lateral interactions of SPM with other membrane lipids and the resulting impact on lateral organization within membranes have received a great deal of attention. Far less clear is the influence that lateral interactions with SPM can have on the transmembrane distributions of neighboring membrane lipids. We recently found that SPM affects the transbilayer distribution of GalCer in SUVs (Mattjus et al., 2002). This study examines the structural features required for the SPM molecule to modulate the transbilayer distribution of *N*-palmitoyl-β-GalCer.

From a structural viewpoint, SPM and phosphatidylcholine (PC) share many similarities but do have important differences (Fig. 1). The zwitterionic polar headgroup of SPM, like that of PC, is phosphocholine. Although SPM and PC both have two long nonpolar hydrocarbon chains, they differ with respect to the type of linkage between the long chains and the backbone. In PC, both hydrocarbon chains are generally ester-linked to a glycerol backbone, the *sn*-1 chain usually is saturated (e.g., palmitate or stearate), and the *sn*-2 chain usually contains one or more *cis* double bonds. In contrast, in SPM, the sphingoid base serves the dual role as both the interfacial backbone and nonpolar hydrocarbon chain and the single acyl chain is amide-linked and tends to be saturated. The abundance of long, saturated *N*-acyl chains in SPM provides a marked intramolecular chain-length asymmetry. In

Submitted November 24, 2004, and accepted for publication January 10, 2005.

Barbara Malewicz and Jacob T. Valiyaveettil contributed equally to this work.

Address reprint requests to Rhoderick E. Brown, E-mail: rebrown@hi.umn.edu or reb@umn.edu; or Robert Bittman, E-mail: robert_bittman@qc.edu.

Peter Mattjus's present address is Åbo Akademi University, Dept. of Biochemistry and Pharmacy Artillerigatan 6 A III, BioCity (PO Box 66), FIN-20520 Turku, Finland.

Abbreviations used: SPM, sphingomyelin; POPC, 1-palmitoyl-2-oleoyl-*sn*-glycero-3-phosphocholine; GalCer, galactosylceramide; SUVs, small unilamellar vesicles; DPPC, 1,2-palmitoyl-*sn*-glycero-3-phosphocholine; DMPE, 1,2-myristoyl-*sn*-glycero-3-phosphoethanolamine; DPPE, 1,2-palmitoyl-*sn*-glycero-3-phosphoethanolamine; dihydroSPM, *N*-palmitoyl-4,5-dihydrosphingosylphosphorylcholine; 3-deoxySPM, 3-deoxy-*N*-palmitoyl-sphingosylphosphorylcholine; 1-alkyl-2-amido PC, 1-*O*-hexadecyl-2-deoxy-palmitoylamido-*sn*-glycero-3-phosphocholine; TNBS, trinitrobenzenesulfonate; GlcCer, glucosylceramide.

0006-3495/05/04/2670/11 $2.00

doi: 10.1529/biophysj.104.057059

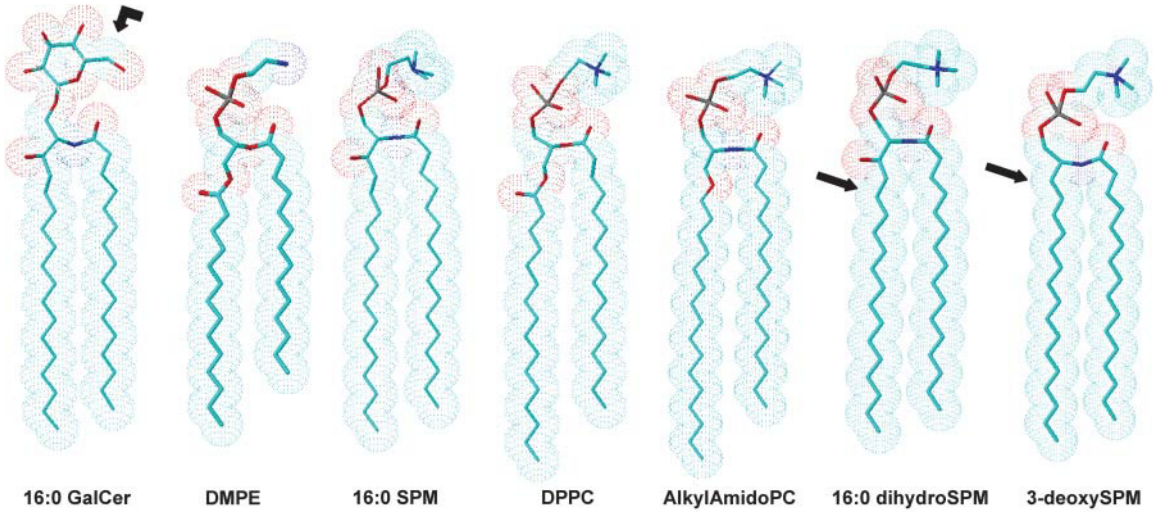

FIGURE 1 Structural features of GalCer, DMPE, SPM, dipalmitoyl-PC, 1-alkyl-2-amido phosphatidylcholine, dihydroSPM, and 3-deoxySPM. Blue represents nitrogen atoms and red represents oxygen atoms. For simplicity, the hydrocarbon chains are depicted as fully extended *trans*-rotamers. In reality, free rotation about the carbon-carbon single bonds produces *trans-gauche* isomerization which occurs at higher frequency in the fluid state compared to the gel state. As is illustrated, matching of chain lengths among the sphingoid- and glycerol-based lipids is optimal when the glycerol-based lipids contain myristoyl *sn*-1 chains. The arrow for GalCer indicates the position of ^{13}C enrichment. The arrow for the dihydroSPM indicates the position where saturation of the 4,5-*trans* double bond has occurred. The arrow for 3-deoxySPM indicates the position of the missing hydroxy group.

addition, the sphingoid chain of SPM possesses a hydroxyl group and a *trans* double bond. These interfacial functional groups affect hydration and hydrogen bonding capacity with surrounding water and/or neighboring lipids. Although the structural features of SPM significantly affect lateral interactions with other membrane lipids such as cholesterol (Brown, 1998; Ohvo-Rekilä et al., 2002; Silvius, 2003), their importance in modulating glycosphingolipid transmembrane distributions remains largely unknown.

In our previous study of the transmembrane distribution of monoglycosylceramide (Mattjus et al., 2002), we showed how ^{13}C- and ^{31}P-NMR spectroscopy can be used to quantitatively assess the transbilayer distributions of all lipids in the SUVs, i.e., GalCer, SPM, and POPC. A significant change was observed in the transbilayer distribution of GalCer in SPM/POPC compared to POPC vesicles, which we refer to as the ''SPM effect''. The goal of this study was to identify sphingolipid structural elements responsible for the SPM effect. We have found that both the *trans*-4,5-double bond and 3-hydroxy group must be present in the sphingoid base for SPM to observe the SPM effect. Also, incorporation of a glycerophospholipid containing an amide-linked chain in place of one of the ester-linked chains in the POPC vesicles did not alter the GalCer transbilayer distribution. Our findings indicate that subtle changes in the hydration/hydrogen bonding networks associated with the lipid headgroup and interfacial regions of the different SPM derivatives affect interactions with GalCer and suggest that lateral interactions between monoglycosylceramide and SPM are important for controlling the transbilayer distributions of simple glycolipids in curved membranes.

MATERIALS AND METHODS

Materials

[6-^{13}C]Galactose (99 atom-% ^{13}C) was obtained from Omicron Biochemicals (South Bend, IN) and used to synthesize [6-^{13}C]GalCer (99.8% isotopic enrichment) as described by Mattjus et al. (2002). POPC, DMPE, DPPE, DPPC, and egg and milk SPM were obtained from Avanti Polar Lipids (Alabaster, AL). Lipid purity was confirmed by high resolution ^{31}P- and ^{13}C-NMR (Malewicz and Baumann, 1996; Mattjus et al., 2002). The sphingoid base composition of the egg SPM used in this study was >99% sphingenine and had no detectable sphinganine base, whereas the milk SPM contained 83% sphingenine and 17% sphinganine base as characterized by their respective ^{31}P-NMR resonances at 0.69 ppm (4-sphingenine = sphingosine) and at 0.91 ppm (sphinganine = dihydrosphingosine; Ferguson et al., 1996). DihydroSPM was synthesized by catalytic hydrogenation of sphingosylphosphorylcholine followed by *N*-acylation with *p*-nitrophenyl palmitate. 3-Deoxy-*N*-palmitoyl-SPM was synthesized as described previously (Byun et al., 1998). 1-*O*-Alkyl-2-amido-PC was synthesized from D-mannitol via the intermediates 1-*O*-hexadecyl-2,3-isopropylidene-*sn*-glycerol and 1-*O*-hexadecyl-2-azido-*sn*-glycerol. Deuterated solvents ($CDCl_3$, CD_3OD, D_2O) were obtained from Cambridge Isotope Laboratories (Andover MA). GalCer was quantified gravimetrically.

Nuclear magnetic resonance

Nuclear magnetic resonance (NMR) analyses were performed using a Varian UNITY 300 instrument (Varian Associates, Palo Alto, CA) equipped with a 5-mm variable temperature probe. NMR spectra of vesicles and of lipid solutions were acquired at 37°C and 25°C, respectively. For vesicles, proton-decoupled ^{31}P-NMR and ^{13}C-NMR spectra were recorded as described by Mattjus et al. (2002). ^{31}P-NMR analysis of phospholipid solutions were performed in $CDCl_3/CD_3OD/D_2O$ (50:50:15) as described earlier (Malewicz and Baumann, 1996). Spectra were referenced relative to concentrated H_3PO_4 for ^{31}P-NMR and tetramethylsilane for ^{13}C-NMR.

Vesicle preparation

SUVs were prepared by sonication using a modification of the established procedure by Huang and Thompson (1974) and described in detail by Mattjus et al. (2002). Immediately after preparation, the vesicles were used for NMR analysis. The phospholipid concentration of the vesicle preparations was confirmed by solution ^{31}P-NMR. For that purpose, 100 μl of each vesicle preparation was dissolved in 0.7 ml of $CDCl_3$:CD_3OD (1:1 by volume), and individual phospholipids were quantified (Malewicz and Baumann, 1996). Vesicle stability and impermeability to ions were ascertained by monitoring the ^{31}P-NMR chemical shifts and signal intensities of the phospholipids as a function of time. By these criteria, all vesicles used in this study remained stable and ion-impermeable for several days.

Assessment of GalCer localization in vesicles by ^{13}C-NMR

GalCer was localized and quantified in the inner and outer leaflets of POPC and POPC/SPM vesicles by ^{13}C-NMR using ^{13}C-enriched GalCer as described previously (Mattjus et al., 2002). Briefly, vesicles composed of phospholipids and [6-^{13}C]GalCer were analyzed by quantitative ^{13}C-NMR in the absence and presence of 5 mM Mn^{2+}. This concentration of Mn^{2+} was sufficient to cause complete relaxation of the C-13 resonances derived from GalCer in the outer leaflet of the SUVs without inducing membrane permeability changes or vesicle aggregation. Thus, the integral of [6-^{13}C]GalCer resonance at 61.361 ppm obtained in the absence of the relaxing reagent represents the total of GalCer molecules, whereas the integrals determined in the presence 5 mM Mn^{2+} represent the GalCer molecules localized in the inner leaflet of the SUVs.

Assessment of phospholipid localization in vesicles

Phospholipid transbilayer distributions in vesicles were determined by ^{31}P-NMR using praseodymium (Pr^{3+}) as described previously (Kumar et al., 1988). Briefly, when 1 mM Pr^{3+} was added to vesicles, the ^{31}P-NMR resonances derived from the outer leaflet phospholipid molecules were shifted downfield, whereas the resonances derived from the inner leaflet phospholipid molecules remained unchanged as long as vesicle integrity is maintained. Integration of both resonances allowed precise determination of phospholipid outside-to-inside molar ratios. This procedure was used for POPC/PE, POPC/SPM, or POPC with a SPM analog because their respective chemical shifts differed sufficiently to observe individual resonances. To confirm that 5 mM Mn^{2+} completely quenched the resonances originating from the vesicle outer leaflets and that vesicle integrity was maintained in the presence of paramagnetic ions, the following control experiments were performed. ^{31}P-NMR spectra of PC vesicles were acquired in the presence of 1 mM Pr^{3+}, causing a downfield shift of the PC outer leaflet resonance peak (10.258 ppm). The inner leaflet resonance (−0.900 ppm) was not affected by the external Pr^{3+}. Subsequent addition of 5 mM Mn^{2+} to these vesicles completely quenched the outer leaflet PC resonance (10.258 ppm) without affecting the inner leaflet PC resonance (−0.900 ppm), thus confirming the efficacy of 5 mM Mn^{2+} for completely quenching the outer leaflet resonances. The unquenched inner leaflet resonance remained stable and unchanged for several days after addition of Pr^{3+} and Mn^{2+}, verifying vesicle integrity under our experimental conditions.

When vesicles were composed of three phospholipids with small differences in their ^{31}P-NMR chemical shifts, additional methodology was employed. For example, in POPC/SPM/PE SUVs, the ^{31}P-NMR resonance signal of POPC was well resolved from those of SPM and PE, but the signals of SPM and PE were not well separated from each other, in agreement with an earlier report (Warschawski et al., 1996). Thus, in POPC/SPM/PE SUVs, only the inner and outer leaflet distributions of POPC could be determined using the paramagnetic shift reagent, Pr^{3+}. Establishing the transbilayer distribution of SPM in the POPC/SPM/PE SUVs required the additional application of ^{13}C-NMR to measure the transbilayer distribution of the choline methyl resonances of the SPM and POPC headgroups (Fig. 2). The ^{13}C-NMR approach was feasible because the choline methyl resonances of the outer and inner leaflets of the POPC/SPM/PE (45:45:10) SUVs were well resolved from each other in the absence of Mn^{2+} (Fig. 2 *A*). The downfield choline methyl resonance (54.9 ppm) was assigned to SPM/POPC comprising the outer leaflet on the basis of sensitivity to Mn^{2+}, whereas the resonance at 54.5 ppm was assigned to inner leaflet SPM/POPC choline methyl residues because this signal was not affected by external Mn^{2+} (Fig. 2 *B*). The SPM transbilayer distribution then could be deduced from the ^{13}C-NMR data because the POPC transbilayer distribution could be independently established by ^{31}P-NMR. Unfortunately, the methylene carbon resonances of the PE ethanolamine were not sufficiently resolved from those of the SPM/POPC choline groups to allow the preceding strategy to be used to determine the transbilayer distribution of PE when SPM was present. However, establishment of the SPM transbilayer distribution enabled the PE contribution to the unresolved SPM/PE ^{31}P-NMR resonance signals to be accurately calculated when the vesicles contained sufficiently high PE (e.g., 10 mol %).

To independently quantitate the PE transbilayer distribution in POPC/SPM/PE vesicles, PE was chemically labeled with TNBS (Litman, 1974; Nordlund et al., 1981). An advantage of using TNBS is its sensitivity, permitting low PE concentrations (e.g., 1 mol %) to be accurately determined. At higher PE mole fractions (e.g., 10 mol %) in POPC vesicles, side by side comparisons showed good agreement between the TNBS and ^{31}P-NMR approaches for quantifying the transmembrane distribution of PE.

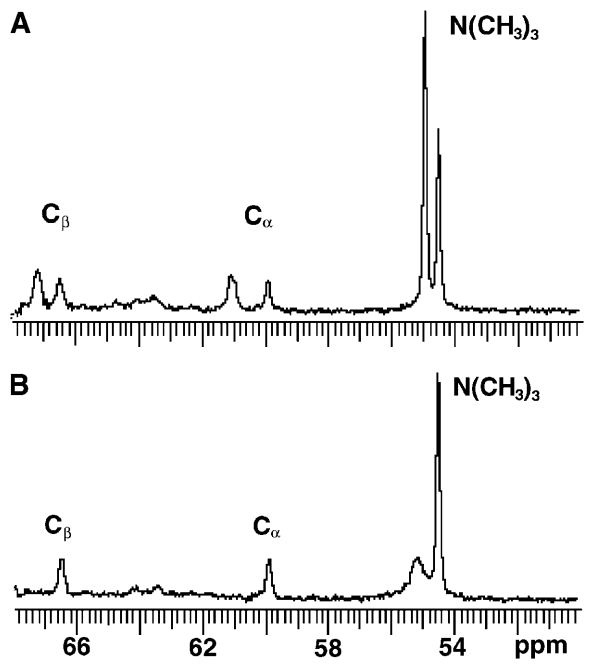

FIGURE 2 ^{13}C-NMR assessment of the transbilayer distribution of SPM and POPC from the headgroup choline methyl resonances. On the basis of sensitivity to Mn^{2+} (*Panel A*), the upfield choline methyl resonance (54.9 ppm) was assigned to outer leaflet SPM/POPC, whereas the resonance at 54.5 ppm was assigned to inner leaflet choline methyl residues of SPM/POPC; the latter signal was not affected by external Mn^{2+}. Panel *B* shows the choline resonances of the outer and inner leaflets of POPC/SPM/PE (45:45:10) SUVs in the absence of Mn^{2+}.

RESULTS

We showed previously that GalCer at low concentrations in POPC vesicles (1 or 2 mol %) preferentially localizes to the vesicle inner leaflet (~70%) and that incorporation of egg SPM into the vesicles dramatically changes the transbilayer distribution of GalCer (Mattjus et al., 2002). To rule out the possibility that the 70% inner leaflet preference of GalCer is an artifact of having extremely low GalCer concentration in the POPC vesicles, we performed the NMR analyses using 5 mol % [6-^{13}C]-GalCer in POPC SUVs. We found that 74.6 mol % of the [6-^{13}C]-GalCer was localized to the inner leaflet, whereas 25.4 mol % of the glycolipid localized to the outer leaflet.

Does SPM alter the transmembrane distribution of disaturated PEs?

To determine whether SPM has the capacity to modulate the transbilayer distribution of nonsphingoid-based membrane lipids with overall molecular shapes resembling GalCer, the transbilayer distributions of DMPE and DPPE were assessed in POPC and SPM/POPC SUVs. Among glycerol-based lipids, DMPE and DPPE were chosen because they have relatively small, low hydration capacity headgroups and saturated acyl chains, which render their overall molecular shapes similar to that of 16:0 GalCer. To establish whether the signal resonances of PE, POPC, and egg SPM could be resolved sufficiently to permit quantitation by NMR, ^{31}P-NMR measurements were performed on DMPE/POPC (1:9) and DMPE/POPC/egg SPM (10:45:45) SUVs using Pr^{3+} ions to shift the outer leaflet phosphorus signals of DMPE, POPC, and SPM. Fig. 3, *A* and *B*, show the ^{31}P-NMR spectra of control SUVs composed of either POPC/SPM (1:1) or POPC/DMPE (9:1) in the presence of 1 mM Pr^{3+}. Four distinct phosphorus resonances are evident in each spectrum, consistent with previous reports (Castellino, 1978; Mattjus et al., 2002; Schmidt et al., 1977). In Fig. 3 *A*, the resonances at −0.900 and −0.246 ppm represent POPC and SPM of the SUV inner leaflet, whereas the resonances at 5.203 and 7.596 ppm represent outer leaflet-POPC and -SPM that have been shifted downfield by Pr^{3+}. Similarly, in Fig. 3 *B*, the Pr^{3+}-shifted resonances observed for POPC and DMPE in the outer leaflet are well separated from each other, permitting accurate calculation of transbilayer distribution of both phospholipids. Integration of the ^{31}P-NMR peaks in Fig. 3, *A* and *B* revealed that SPM displays a slight preference for the outer leaflet of the POPC/SPM vesicles but that DMPE prefers the inner leaflet in POPC/DMPE vesicles. The findings are in general agreement with previously reported distributions of SPM and other PE species in PC SUVs (Castellino, 1978; Nordlund et al., 1981; Williams et al., 2000).

^{31}P-NMR spectra of POPC/SPM/DMPE (45:45:10 mol %) SUVs, recorded in the presence of Pr^{3+} ions (Fig. 3 *C*), show that the ^{31}P-NMR resonances of SPM and DMPE coalesce and could not be resolved within either vesicle leaflet. Contributing to the poor resolution of the SPM/DMPE inner leaflet resonance from the POPC inner leaflet resonance were the increased line widths ($\nu_{1/2}$), indicating restricted mobility of all phospholipids molecules. Whereas $\nu_{1/2}$ values measured for inner leaflet POPC in POPC/SPM (Fig. 3 *A*) and in POPC/DMPE SUVs (Fig. 3 *B*) were 24 and 20 Hz, respectively, the value increased to 149 Hz in POPC/SPM/DMPE SUVs (Fig. 3 *C*). Likewise, the values of $\nu_{1/2}$ measured for inner leaflet SPM and DMPE were 36.5 and 14.0 Hz, respectively, when each was introduced into POPC SUV separately (Fig. 3, *A* and *B*). However, the value for the inner leaflet SPM/DMPE resonance in POPC/SPM/DMPE SUVs increased to 185 Hz (Fig. 3 *C*). Although resonance line broadening also was observed for the outer leaflet of the SUVs, detailed quantification was not pursued because Pr^{3+} is known to induce line broadening of outer leaflet resonances. The total outside-to-inside phosphorus ratios of 1.94, 2.03, and 1.80 for the POPC/DMPE, POPC/SPM, and POPC/SPM/DMPE vesicles, respectively, were consistent with the vesicles having diameters of 35 nm or less (Huang and Thompson, 1974; Lichtenberg and Barenholz, 1988). Nonetheless, the simultaneous determination of the POPC, SPM, and DMPE transbilayer distributions in the three component vesicles was not feasible by ^{31}P-NMR spectroscopy.

Because the DMPE and SPM signals in POPC/SPM/DMPE vesicles could not be resolved from each other by ^{31}P-NMR, an alternative ^{13}C-NMR experimental strategy was

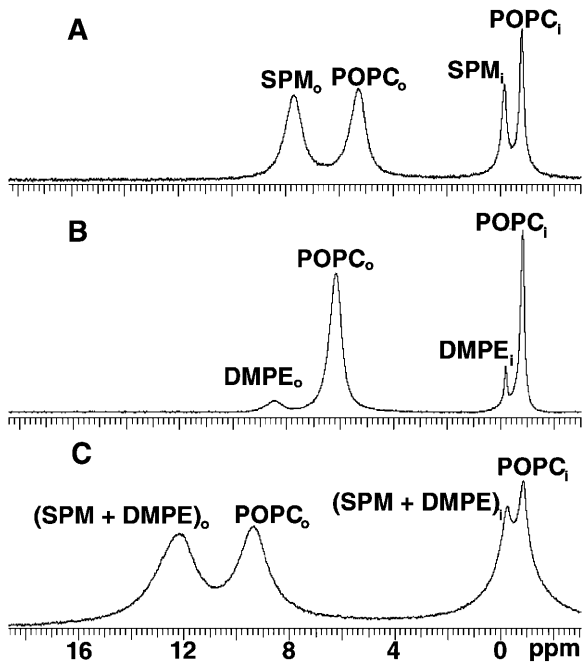

FIGURE 3 ^{31}P-NMR spectra of POPC/SPM, POPC/DMPE, and POPC/SPM/DMPE vesicles. The spectra were acquired in the presence of 1 mM Pr^{3+}. Panel *A* shows SUVs composed of equimolar POPC/SPM. Panel *B* shows SUVs composed of POPC/DMPE (9:1). Panel *C* shows SUVs composed of POPC/SPM/DMPE (45:45:10).

used, as described in full in Materials and Methods. This strategy permitted quantitative determination of the SPM and PE transbilayer distributions in the POPC/SPM/DMPE vesicles when the PE mole fraction was sufficiently high (e.g., 10 mol %), but was inadequate at low PE mole fractions (e.g., 1 mol %). To circumvent this problem, the amino-specific and bilayer impermeant chemical labeling agent, TNBS, was used to quantify the transmembrane distribution of DMPE in SPM/POPC vesicles. Before using TNBS with DMPE/SPM/POPC vesicles, we performed control experiments to confirm the efficacy of the approach. DMPE clearly showed an inner leaflet preference compared to POPC in DMPE/POPC (1:9) vesicles (Table 1), in agreement with the ^{31}P-NMR data. This inner leaflet preference of DMPE persisted even when the DMPE content was lowered to either 5 or 1 mol %. DPPE was also localized preferentially in the inner leaflet of POPC SUVs (data not shown). Having confirmed the agreement between the TNBS and ^{31}P-NMR approaches for localizing DMPE in DMPE/POPC (1:9) vesicles, we examined the effect of including SPM in the vesicles. Incorporation of 45 mol % SPM into the POPC SUVs produced almost no change in the distribution of DMPE (Table 1) compared with its distribution in POPC SUVs, regardless of whether the mole fraction of DMPE was 0.1 or 0.01. The findings are noteworthy because they markedly contrast with those of 16:0 GalCer (1 or 2 mol %), which localizes predominantly (70%) in the inner leaflet of POPC SUVs but is significantly redistributed in the presence of SPM.

Is the transbilayer distribution of GalCer in phospholipid vesicles affected by DPPC or by 1-alkyl-2-amido PC?

To establish whether membrane lipids that share structural similarities with SPM also have the capacity to alter the transbilayer distribution of GalCer in phospholipid vesicles, we replaced the egg SPM in POPC/SPM vesicles with DPPC. This phosphoglyceride has saturated acyl chains, a phosphocholine headgroup, and a similar phase transition temperature as 16:0-SPM, the major constituent (~85%) of egg SPM. Before measuring the transbilayer distribution of [6-^{13}C] GalCer in POPC/DPPC, we confirmed that 5 mM Mn^{2+} completely quenches the ^{31} P resonances originating from the vesicle outer leaflet and that vesicle integrity remains intact (see Materials and Methods).

To determine if DPPC could alter the transmembrane distribution of [6-^{13}C]-GalCer, ^{13}C-NMR spectra were recorded with POPC/DPPC/[6-^{13}C]-GalCer (49.5:49.5:1) SUVs in the absence and presence of 5 mM Mn^{2+} (Fig. 4, *A* and *B*). Analysis of the spectra indicated that 70.2 mol % of the [6-^{13}C]GalCer is localized in the SUV inner leaflet. This [6-^{13}C]-GalCer distribution was nearly identical to that observed in POPC SUVs containing no DPPC (see Fig. 7) and differed significantly from the 48.4 mol % inner leaflet localization of [6-^{13}C]GalCer observed in SUVs composed of equimolar POPC/egg SPM.

To determine whether the amido linkage in SPM might be responsible for the ability of SPM to alter the GalCer transbilayer distribution, we incorporated 1-alkyl-2-amido PC into POPC SUVs. This phosphoglyceride contains all of the structural features of DPPC as well as hydrocarbon linkages that more closely resemble those of SPM. However, in vesicles composed of POPC/1-alkyl-2-amido PC/[6-^{13}C]-GalCer (66:33:1), we observed no change in the GalCer transbilayer distribution compared with control POPC/[6-^{13}C]-GalCer (98:2) vesicles (see Fig. 7).

Which functional groups of SPM are important for modulation of the transbilayer distribution of GalCer in phospholipid vesicles?

Because the 3-hydroxy group and the 4,5-*trans* double bond in the sphingoid base chain of SPM have been implicated in the lateral interactions between SPM and cholesterol (Ramstedt and Slotte, 2002; Silvius, 2003), we evaluated the importance of these functional groups for enabling SPM to modulate the transbilayer distribution of GalCer. Before

TABLE 1 PE transbilayer distributions in POPC and POPC/SPM vesicles

	POPC		SPM		GalCer		DMPE	
Vesicle composition	Outer	Inner	Outer	Inner	Outer	Inner	Outer	Inner
POPC/GalCer (99:1)	66.0	34.0			29.9	70.1		
POPC/SPM (50:50)	64.3	35.7	70.3	29.7				
POPC/SPM/GalCer (49.5:49.5:1)	65.8	34.2	72.4	27.6	51.6	48.4		
POPC/DMPE* (90:10)	68.1	31.9					47.3	52.7
POPC/SPM/DMPE* (45:45:10)	60.3	39.7	65.7	34.3			51.4	48.6
POPC/DMPE* (99:1)	65.9	34.1					53.3	46.5
POPC/SPM/DMPE** (49.5:49.5:1)	62.6	37.4	65.8	34.2			49.3	50.7

The values for the outer and inner leaflets are listed as percentages. The typical standard errors associated with our SUV preparations are 1%–2% of the values shown. The transbilayer distributions for POPC, SPM, and GalCer were determined by NMR. The data for the POPC/GalCer and POPC/SPM/GalCer vesicles are values obtained with different batches of lipids and vesicles and confirm previous observations (Mattjus et al., 2002).

*Determination of the DMPE transbilayer distribution by both NMR and TNBS.

**Determination of the DMPE transbilayer distribution only by TNBS.

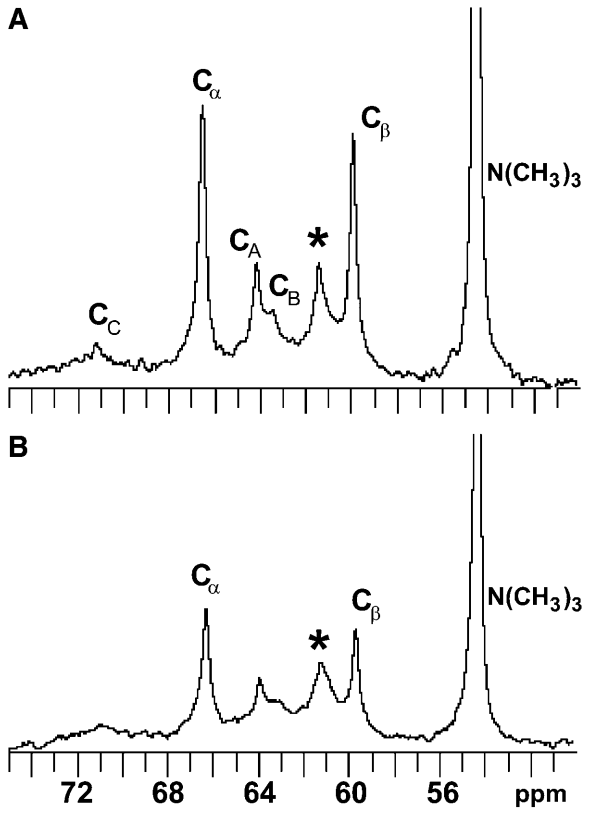

FIGURE 4 ^{13}C-NMR spectra of POPC/DPPC/[6-^{13}C]GalCer (49.5:49.5:1) vesicles in the absence (*A*) and presence (*B*) of 5 mM Mn^{2+}. C_A, C_B, and C_C indicate the resonances of the glycerol carbons, and C_α and C_β indicate the phosphocholine headgroup resonances. The asterisk indicates the [6-^{13}C] resonance of galactose.

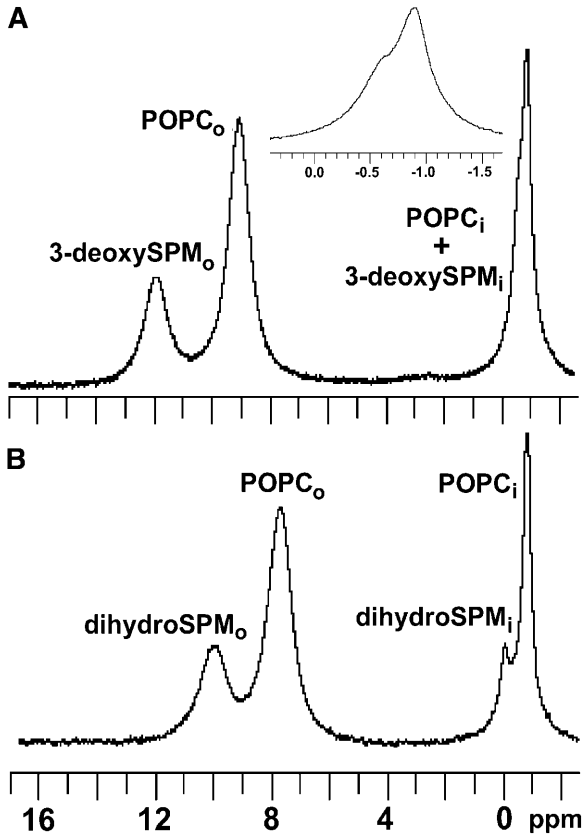

FIGURE 5 ^{31}P-NMR spectra of POPC/3-deoxySPM/GalCer (66:33:1) vesicles (*A*) and POPC/dihydroSPM/[6-^{13}C]GalCer (66:33:1) vesicles (*B*) in the presence of 1 mM Pr^{3+}. An expanded view of the chemical shifts (*panel A*, *inset*) shows the 3-deoxySPM (0.63 ppm) shoulder on the POPC (0.90 ppm) peak.

determining the transbilayer distribution of [6-^{13}C]GalCer in the SPM analog/POPC vesicles, the transbilayer distributions of 3-deoxy-*N*-palmitoyl-SPM and dihydroSPM were established by ^{31}P-NMR. Fig. 5 shows the ^{31}P-NMR spectra of vesicles comprised of POPC/3-deoxySPM/GalCer (66:33:1; Fig. 5 *A*) and POPC/dihydroSPM/GalCer (66:33:1; Fig. 5 *B*) in the presence of 1 mM Pr^{3+}. The external paramagnetic ion caused downfield shifts of the outer leaflet resonances of POPC and of the SPM derivatives but did not affect the inner leaflet resonances of POPC, 3-deoxySPM, or dihydroSPM. Whereas the dihydroSPM resonance was well resolved from the POPC resonance (−0.20 and −0.90 ppm, respectively), the ^{31}P-NMR resonance of 3-deoxySPM was in close proximity (−0.63 ppm) to that of POPC (Fig. 5 *A*, *inset*), but could be quantified after resonance deconvolution. Analysis of the transbilayer distributions of POPC and SPM analogs showed a slight preference of the SPM analogs for the outer leaflet (see Fig. 7). The total outside-to-inside phosphorus ratios were 1.80 and 1.88, respectively, for the POPC/3-deoxySPM/GalCer (66:33:1) and POPC/dihydroSPM/GalCer (66:33:1) vesicles, consistent with their diameters being 35 nm or less (Huang and Thompson, 1974; Lichtenberg and Barenholz, 1988).

Having observed no significant difference in the transbilayer distributions of 3-deoxySPM, dihydroSPM, and SPM in the similarly sized SUVs (see Fig. 7), we next addressed the issue of whether either SPM analog affected the transbilayer distribution of GalCer. ^{13}C-NMR spectra of POPC/3-deoxySPM/[6-^{13}C]GalCer (66:33:1) and POPC/dihydroSPM/[6-^{13}C]GalCer (66:33:1) SUVs in the absence and presence of 5 mM Mn^{2+} are displayed in Fig. 6, *A* and *B*. Analyses of the spectra indicated that ~71 mol % of the [6-^{13}C]GalCer remained localized in the vesicle inner leaflets (Fig. 7), comparable to the GalCer distribution observed in control POPC/[6-^{13}C]-GalCer (99:1) vesicles, but substantially different from the 54.1 mol % inner leaflet localization of [6-^{13}C]GalCer observed in POPC/egg SPM/GalCer (66:33:1) vesicles.

Since neither 3-deoxySPM nor dihydroSPM altered the GalCer transbilayer distribution of GalCer in POPC vesicles, additional experiments were performed to better understand why egg SPM is capable of altering the GalCer transbilayer distribution in POPC SUVs. We evaluated whether the acyl composition heterogeneity of SPM could be responsible for the SPM effect by performing two complementary

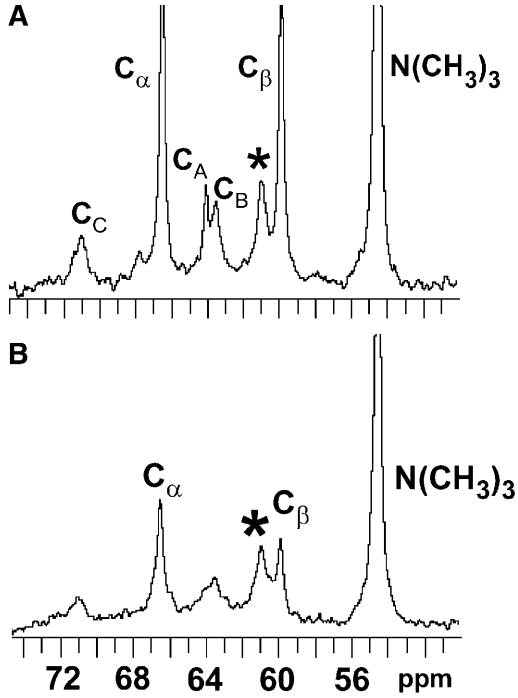

FIGURE 6 ^{13}C-NMR spectra of POPC/dihydroSPM/[6-^{13}C]-GalCer (66:33:1) vesicles in the absence (*A*) and presence (*B*) of 5 mM Mn^{2+}. C_A, C_B, and C_C indicate the resonances of the glycerol carbons, and C_α and C_β indicate the phosphocholine headgroup resonances. The asterisk indicates the [6-^{13}C] resonance of galactose.

experiments. First, we used milk SPM instead of egg SPM and determined the transbilayer distribution of GalCer in milk SPM/POPC SUVs. In egg SPM, the dominant fatty acyl chain is palmitate (~85%), whereas in milk SPM, mostly saturated and long chains, i.e., C22 (19%), C23 (33%), and C24 (20%) occur. We found that milk SPM was not able to alter the transbilayer distribution of GalCer (Fig. 8). We also synthesized SPM that contained only an *N*-palmitoyl chain, the predominant acyl chain in egg SPM, and determined the GalCer transbilayer distribution in 16:0-SPM/POPC SUVs. POPC vesicles containing 16:0-SPM duplicated the results obtained with egg SPM.

The lack of correlation between acyl chain heterogeneity and the SPM effect led us to evaluate the dihydrosphingosine base content of our preparations of milk SPM and egg SPM in solution by ^{31}P-NMR. We determined that the milk SPM contained 17 mol % of 4,5-dihydro sphingoid base but that our egg SPM contained no detectable dihydroSPM (see Materials and Methods). This finding suggested the possibility that the dihydroSPM content may be a key determinant in controlling whether naturally occurring SPMs alter GalCer transbilayer distribution in POPC vesicles. To test this possibility, we performed a series of experiments in which different amounts of *N*-palmitoyl-dihydroSPM replaced a portion of egg SPM in POPC/egg SPM/GalCer (49.5:49.5:1) vesicles. Raising the dihydroSPM content to 10 mol % or higher completely abrogated the capacity of egg SPM to alter the transbilayer distribution of GalCer in POPC/SPM vesicles and incorporation of as little as 2 mol % dihydroSPM had a mitigating effect (Fig. 8).

DISCUSSION

The results of this study suggest that the dramatic change in the transbilayer distribution of GalCer caused by SPM in POPC SUVs has a remarkably high degree of structural specificity. Analogs that share many of the structural features of GalCer and SPM are not capable of duplicating the effect of the authentic parent molecules. DMPE, which roughly

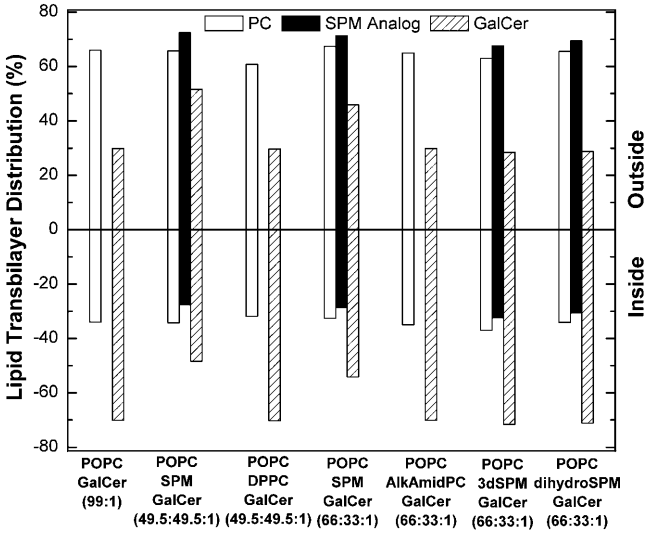

FIGURE 7 Outer and inner leaflet distributions of GalCer, SPM, SPM analogs, and other phospholipids. The vesicles contained 1 mol % GalCer.

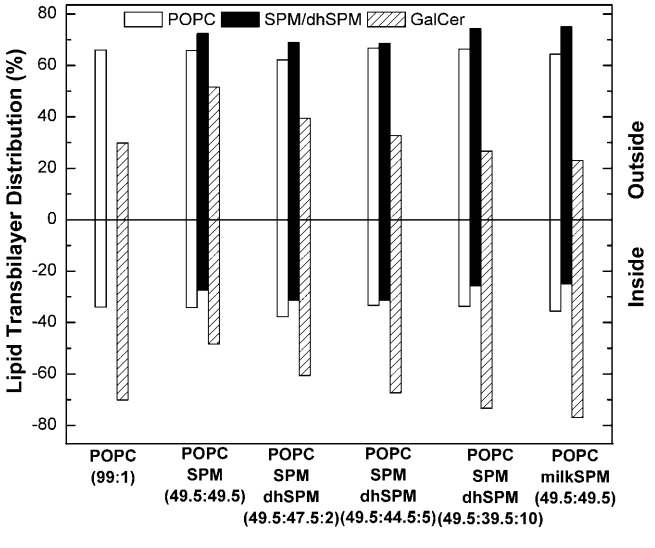

FIGURE 8 Effect of increasing amounts of dihydroSPM on the transbilayer distribution of GalCer in POPC/SPM/GalCer (66:33:1) vesicles. The vesicles contained 1 mol % GalCer.

mimics some of the features of GalCer (a relatively nonbulky, low hydration capacity headgroup, and saturated acyl chains; Hinz et al., 1985; Koynova et al., 1988), is enriched in the inner leaflet (47%–54%) of POPC/DMPE SUVs (9:1) compared to POPC (32%–34% inner leaflet). In contrast to GalCer, the DMPE inner leaflet localization is not affected by incorporation of egg SPM into the vesicles (Table 1). In the one previous study in which NMR was used to assess the transbilayer distribution of PE in vesicles comprised of equimolar egg PC and PE (Berden et al., 1975), 46 mol % of the PE was found in the inner leaflet, but the effect of SPM was not investigated. We observed the inner leaflet preference of DMPE even at low PE mole fractions (<10 mol %). This finding was unexpected because earlier reports indicated that the inner leaflet preference of PE in SUVs does not become apparent until the PE content exceeds ~10 mol % (Nordlund et al., 1981). In the earlier studies, egg PE was used rather than DMPE, perhaps accounting for the difference. In our view, the preference of DMPE for the inner leaflet of POPC SUVs is not surprising. Other phosphoglycerides with relatively small headgroups, such as phosphatidylethanol, strongly prefer the inner leaflet of DOPC SUVs when present at low mole fractions (Victorov et al., 1996; 1997). *N*-Palmitoyl-GalCer displays a similar inner leaflet preference in POPC SUVs under identical conditions (Mattjus et al., 2002). Our results also show that SPM displays no capacity to alter the transbilayer distribution of DMPE, even though DMPE shares general similarities with *N*-palmitoyl GalCer with respect to headgroup size, hydration, and molecular shape.

A second noteworthy outcome of this study was the identification of the essential SPM structural features that enable this sphingolipid to alter the transbilayer distribution of GalCer in high-curvature POPC vesicles. Replacing the SPM in POPC/SPM vesicles with a structurally similar PC (e.g., DPPC or 1-alkyl-2-amido PC) or with a SPM analog (e.g., 3-deoxy SPM or dihydroSPM) completely abrogated the change in GalCer transbilayer distribution produced by SPM. The inability of DPPC to elicit a response is noteworthy because this lipid is often used as a SPM analog in studies of raft lipid interactions. The PC species used in this study share considerable structural similarity with 16:0 SPM (Fig. 1), the dominant constituent (~85%) of egg SPM. Both PC and SPM have phosphocholine headgroups, which are oriented approximately parallel to the bilayer interface (Khare and Worthington, 1978). The glycerol backbone of PC is configurationally analogous to the initial three carbons of the 18-carbon sphingoid base of SPM (Pascher et al., 1992). The remaining 15 carbons of the sphingoid base, which include a 4,5-*trans* double bond, are structurally similar to the saturated palmitoyl *sn*-1 chain of DPPC and the alkyl chain of 1-alkyl-2-amido PC. The *sn*-2 acyl chain of DPPC and the *N*-linked acyl chain of 1-alkyl-2-amido PC and of SPM share a similar conformation in that their first two carbons of the chains extend roughly parallel to the bilayer interface but the chains then bend sharply to become more aligned with the respective *sn*-1 acyl chain or sphingoid base (Hamilton et al., 1993; Pascher et al., 1992; Ruocco et al., 1996). The result is axial displacement of the carbon atoms of the two intramolecular chains and positional inequivalence along the chains (Fig. 1). Despite the preceding similarities in overall conformation and shape of DPPC, 1-alkyl-2-amido PC, and 16:0-SPM, our NMR data clearly show that the change in the transbilayer distribution of GalCer induced by SPM in POPC/SPM vesicles is not duplicated by DPPC or by 1-alkyl-2-amido PC. This finding emphasizes the importance of the functional groups that distinguish PC and SPM.

The finding that the subtle chemical differences between PC and SPM can manifest themselves in significant ways is supported by other evidence. SPM and PC are known to produce distinct ^{31}P-NMR resonances and Pr^{3+} induces a larger downfield shift for SPM than for PC, consistent with their phosphate groups residing in nonidentical local environments (Castellino, 1978; Schmidt et al., 1977). The hydration features of SPM differ in subtle but important ways compared to PC (Jendrasiak and Smith, 2001; Niemelä et al., 2004). ^{2}H NMR studies of POPC/SPM multilamellar liposomes indicate that an increase in SPM content reduces the orientational ordering of interfacial water, probably by diminishing the fraction of water molecules in the carbonyl region of the bilayer (Steinbauer et al., 2003). Monolayer data collected at surface pressures mimicking the biomembrane environment reveal that SPMs have smaller cross-sectional molecular areas than their respective chain-matched PCs (e.g., Li et al., 2000, 2001, and references therein). ^{14}N NMR and ^{13}C-CP/MAS-NMR measurements indicate that, in the liquid-crystalline phase, the quaternary ammonium headgroup is more rigid in SPM that in PC (Epand, 2003; Siminovitch and Jeffery, 1981). Consistent with the experimental data are molecular dynamics simulations showing that the average cross-sectional molecular area and molecular volume of SPM in fluid phase bilayers are smaller than that of DPPC (Chiu et al., 2003; Niemelä et al., 2004).

Our finding that 3-deoxySPM and dihydroSPM do not affect the transbilayer distribution of GalCer suggests that specific functional groups, e.g., the 3-hydroxy and 4,5-*trans* double bond of the sphingoid base chain, have important roles in modulating interactions with GalCer. Solution NMR studies of the dihydro analogs of SPM and ceramide (Ferguson-Yankey et al., 2000; Li et al., 2002; Talbott et al., 2000), modeling studies of ceramides (Vorobyov et al., 2002), and molecular dynamics simulations of SPM (Chiu et al., 2003; Mombelli et al., 2003; Niemelä et al., 2004) all point toward the important roles that the 3-hydroxy group and 4,5-*trans* double bond play in organizing interfacial water and mediating intramolecular hydrogen bonds via strongly bound water molecules. Elimination of the 4,5-*trans* double bond modifies the hydration of the interfacial region, distorts hydrogen bonding interactions, and affects the 3-hydroxy group conformation in ways that increase molecular packing density and alter the molecular dipole potential (Kuikka et al., 2001;

Yappert and Borchman, 2004). Recent monolayer studies of several ceramide analogs clearly delineate the important and unique contribution of the 4,5-*trans* double bond in regulating the interfacial dipole potential, lateral elasticity, and molecular packing of sphingolipids (Brockman et al., 2004).

In the case of SPM, the presence of the highly hydratable and relatively bulky zwitterion, phosphorylcholine, further affects ceramide behavior. However, it is not the mere presence of phosphorylcholine that is important but rather the overall interaction between phosphorylcholine and its subtending ceramide moiety. In SPM, intramolecular hydrogen bonding involving bridging water molecules appears likely between the hydroxy group at C-3 of the sphingoid base and the bridge oxygen of phosphate (Bruzik et al., 1990; Chiu et al., 2003; Mombelli et al., 2003; Niemelä et al., 2004; Schmidt et al., 1977; Talbott et al., 2000). Such an interaction is consistent with the previously described alterations in the hydration of the SPM headgroup and interfacial region, rigidification of the headgroup region, and reduced molecular cross-sectional area of SPM compared to ''chain-matched'' PCs. Because the sphingoid base of GalCer also contains a 4,5-*trans* double bond and a 3-hydroxy group, similar considerations apply to this glycolipid. However, the less bulky and lower hydration capacity sugar headgroup enhances and stabilizes intermolecular hydrocarbon chain packing (Kulkarni and Brown, 1998; Reed and Shipley, 1989; Ruocco et al., 1981). Because both the 4,5-*trans* double bond and the 3-hydroxy group in the sphingoid base play direct roles in stabilizing the intramolecular hydrogen bonding that restricts headgroup mobility, elimination of either functional group can be expected to affect the balance between intramolecular and intermolecular hydrogen bonding involving SPM and GalCer. The presence of the 4,5-*trans* double bond and the 3-hydroxy group can be expected to enhance the intermolecular interactions between SPM and GalCer, possibly via π-hydrogen bonding involving water that stabilizes the overall interfacial hydrogen bonding network (see Yappert and Borchman, 2004). The conformational flexibility of the DHSPM headgroup, accompanying disruption of the intramolecular hydrogen bonding, might enable DHSPM to compete with GalCer for interaction with SPM, thus explaining the mitigating response of DHSPM on the SPM effect. Further impacting the sphingolipid interactions is the curvature stress associated with each SUV leaflet. Clearly, additional study will be required to elucidate the molecular details of the GalCer-SPM-DHSPM interactions, including the associated impact of positive and negative membrane curvature stress.

Implications

An important issue relates to the relevance of using curvature-stressed membrane vesicles (25–35 nm diameter) to mimic situations existing in cells. Mounting evidence supports the existence of high-curvature membrane structures in cells during certain membrane budding/fission and fusion events (Chernomordik and Kozlov, 2003; Farsad and De Camilli, 2003; Kuhn et al., 2002; Matsuoka et al., 2001). For instance, vesicles formed by inward budding of endosomes, i.e., exosomes, and secreted exocytotically upon fusion of endosomes with the plasma membrane, reportedly have diameters as small as 30 nm (Théry et al., 2002; Wolfers et al., 2001). Also, formation of endocytotic vesicles at the plasma membrane involves proteins that can severely bend membranes (Farsad and De Camilli, 2003). Among the most potent of the curvature-inducing proteins is epsin, which causes liposomes containing phosphatidylinositol-4,5-bisphosphate to form 20-nm diameter bilayer tubules (Ford et al., 2002). Thus, interactions among lipids that occur in high-curvature membrane environments cannot be dismissed a priori as completely irrelevant to the cellular situation but must not be overinterpreted.

Regarding the biological relevance of the SPM analogs used in this study, it should be recalled that dihydroSPM occurs naturally, but varies in concentration among tissues. In egg SPM, the 4,5-dihydro sphingoid base accounts for no more than 7% of the total SPM (Ramstedt et al., 1999). In milk SPM, 15%–20% of the sphingoid base lacks the 4,5-*trans* double bond (Karlsson et al., 1998). However, in SPM of the human eye lens, 77% of the SPM lacks the 4,5-*trans* double bond (Byrdwell and Borchman, 1997). Regulation of the amount of cellular dihydroSPM presumably occurs in the endoplasmic reticulum, where the 4,5-*trans* double bond is introduced into dihydroceramide (Michel et al., 1997). The importance of maintaining the proper balance of the dihydro sphingoid base for membranes is illustrated by the significant biological effects that have been ascribed to the presence of the 4,5-*trans* double bond in sphingolipids, including their ability to act signaling molecules, to enable envelope virus fusion, and to enhance cholesterol solubility in membranes (Corver et al., 1995; Epand, 2003; Kolesnick, 2002; Nyholm et al., 2003). Our findings raise the intriguing possibility that metabolic adjustment of the dihydro/4,5-*trans* double bond ratio in SPM might provide a means to help maintain and/or control the transmembrane distributions of simple sphingolipids and related metabolites in curvature-stressed regions of biomembranes and/or related vesicles. Indeed, an example in which one lipid type affects the transmembrane distribution of another in vivo occurs in transformed murine fibroblasts where uptake of polyunsaturated fatty acids into the plasma membrane alters the transbilayer distribution of sterol (Sweet and Schroeder, 1988).

It should also be noted that GalCer is a lipid of major developmental significance in maturing oligodendrocytes and Schwann cells and of major structural significance during myelination (de Vries and Hoekstra, 2000; van Meer and Lisman, 2002). GalCer is found almost exclusively in the outer myelin leaflet associated with cholesterol in raftlike patches (Simons et al., 2000; Stoffel and Bosio, 1997). The trafficking and recycling of GalCer and SPM in

oligodendrocytes involve endosomal pathways in which cholesterol is known to be enriched in early and recycling endosomes but is relatively depleted in late endosomes. In the plasma membranes of polarized epithelial cells (unstimulated), the apical regions are highly enriched in GlcCer, whereas cholesterol and SPM are found in both the apical and basolateral surfaces (Hoekstra et al., 2003; van Meer and Lisman, 2002). Whether SPM can influence the transbilayer distribution of GlcCer is not known. Also of future interest will be assessment of the effect of cholesterol on the transbilayer distributions of GalCer, GlcCer, and SPM.

We are grateful for support provided by the National Institute of General Medical Sciences-45928 (R.E.B.), the National Heart, Lung, and Blood Institute-16660 (R.B.), the National Institutes of Health RR-04654 (W.J.B.), The Academy of Finland (P.M.), and The Hormel Foundation.

Portions of this investigation were presented in preliminary form at the 48th Annual Meeting of the Biophysical Society held in Baltimore, MD, Feb. 14–18, 2004.

REFERENCES

Andrieu-Abadie, N., and T. Levade. 2002. Sphingomyelin hydrolysis during apoptosis. *Biochim. Biophys. Acta.* 1585:126–134.

Bektas, M., and S. Spiegel. 2004. Glycosphingolipids and cell death. *Glycoconj. J.* 20:39–47.

Berden, J. A., R. W. Barker, and G. K. Radda. 1975. NMR studies of phospholipid bilayers. Some factors affecting lipid distribution. *Biochim. Biophys. Acta.* 375:186–208.

Brockman, H. L., M. M. Momsen, R. E. Brown, L. He, J. Chun, H.-S. Byun, and R. Bittman. 2004. The 4,5-double bond of ceramide regulates its dipole potential, elastic properties, and packing behavior. *Biophys. J.* 87:1722–1731.

Brown, D. A., and E. London. 2000. Structure and function of sphingolipid- and cholesterol-rich membrane rafts. *J. Biol. Chem.* 275:17221–17224.

Brown, R. E. 1998. Sphingolipid organization in biomembranes: What physical studies of model membranes reveal. *J. Cell Sci.* 111:1–9.

Bruzik, K. S., B. Sobon, and G. M. Salamonczyk. 1990. Nuclear magnetic resonance study of sphingomyelin bilayers. *Biochemistry.* 29:4017–4021.

Byrdwell, W. C., and D. Borchman. 1997. Liquid chromatography mass-spectrometeric characterization of sphingomyelin and dihydrosphingomyelin of human lens membranes. *Ophthalmic. Res.* 29:191–206.

Byun, H.-S., J. A. Sadlofsky, and R. Bittman. 1998. Enantioselective synthesis of 3-deoxy-(*R*)-sphingomyelin from (*S*)-1-(4′-methoxyphenyl)-glycerol. *J. Org. Chem.* 63:2560–2563.

Castellino, F. J. 1978. ^{31}P NMR analysis of the surface homogeneity of mixed sphingomyelin-phosphatidylcholine vesicles. *Arch. Biochem. Biophys.* 189:465–470.

Chernomordik, L. V., and M. M. Kozlov. 2003. Protein-lipid interplay in fusion and fission of biological membranes. *Annu. Rev. Biochem.* 72:175–207.

Chiu, S. W., S. Vasudevan, E. Jakobsson, R. J. Mashi, and H. L. Scott. 2003. Structure of sphingomyelin bilayers: a simulation study. *Biophys. J.* 85:3624–3635.

Corver, J., L. Moesby, R. K. Erukulla, K. C. Reddy, R. Bittman, and J. Wilschut. 1995. Sphingolipid-dependent fusion of Semliki Forest virus with cholesterol-containing liposomes requires both the 3-hydroxyl group and the double bond of the sphingolipid backbone. *J. Virol.* 69:3220–3223.

de Vries, H., and D. Hoekstra. 2000. On the biogenesis of the myelin sheath: cognate polarized trafficking pathways in oligodendrocytes. *Glycoconj. J.* 17:181–190.

Edidin, M. 2003. The state of lipid rafts: from model membranes to cells. *Annu. Rev. Biophys. Biomol. Struct.* 32:257–283.

Epand, R. M. 2003. Cholesterol in bilayers of sphingomyelin or dihydrosphingomyelin at concentrations found in ocular lens membranes. *Biophys. J.* 84:3102–3110.

Farsad, K., and P. De Camilli. 2003. Mechanisms of membrane deformation. *Curr. Opin. Cell Biol.* 15:372–381.

Ford, M. G. J., I. G. Mills, B. J. Peter, Y. Vallis, G. J. K. Praefcke, P. R. Evans, and H. T. McMahon. 2002. Curvature of clathrin-coated pits driven by epsin. *Nature.* 419:361–366.

Ferguson, S. R., D. Borchman, and M. C. Yappert. 1996. Confirmation of the identity of the major phospholipid in human lens membranes. *Investig. Ophthalmol. Vis. Sci.* 37:1703–1706.

Ferguson-Yankey, S. R., D. Borchman, K. G. Taylor, D. B. DuPre, and M. C. Yappert. 2000. Conformational studies of sphingolipids by NMR spectroscopy. I. Dihydrosphingomyelin. *Biochim. Biophys. Acta.* 1467: 307–325.

Futerman, A. H., and Y. A. Hannun. 2004. The complex life of simple sphingolipids. *EMBO Rep.* 5:777–782.

Hamilton, K. S., H. C. Jarrell, K. M. Briere, and C. W. M. Grant. 1993. Glycosphingolipid backbone conformation and behavior in cholesterol-containing phospholipid bilayers. *Biochemistry.* 32:4022–4028.

Hinz, H.-J., L. Six, K. P. Ruess, and M. Lieflander. 1985. Head-group contributions to bilayer stability: monolayer and calorimetric studies on synthetic, sterochemically uniform glucolipids. *Biochemistry.* 24:806–813.

Hoekstra, D., O. Maier, J. M. van der Wouden, T. A. Slimane, and S. C. D. van IJzendoorn. 2003. Membrane dynamics and cell polarity: the role of sphingolipids. *J. Lipid Res.* 44:869–877.

Huang, C., and T. E. Thompson. 1974. Preparation of homogeneous, single-walled phosphatidylcholine vesicles. *Methods Enzymol.* 32:485–489.

Jendrasiak, G. L., and R. L. Smith. 2001. The effect of the choline head group on phospholipid hydration. *Chem. Phys. Lipids.* 113:55–66.

Karlsson, A. Å., P. Michélsen, and G. Odham.1998. Molecular species of sphingomyelin: determination by high performance liquid chromatography/mass spectrometry with electrospray and high performance liquid chromatography/tandem mass spectrometry with atmospheric pressure chemical ionization. *J. Mass Spectrom.* 33:1192–1198.

Khare, R. S., and C. R. Worthington. 1978. The structure of oriented sphingomyelin bilayers. *Biochim. Biophys. Acta.* 514:239–254.

Kolesnick, R. 2002. The therapeutic potential of modulating the ceramide/sphingomyelin pathway. *J. Clin. Invest.* 110:3–8.

Koynova, R. D., H. L. Kuttenreich, B. G. Tenchov, and H.-J. Hinz. 1988. Influence of head-group interactions on the miscibility of synthetic, stereochemically pure glycolipids and phospholipids. *Biochemistry.* 27:4612–4619.

Kuhn, R. J., W. Zhang, M. G. Rossmann, S. V. Pletnev, J. Corver, E. Leuches, C. T. Jones, S. Mukhopadhyay, P. R. Chipman, E. G. Strauss, J. S. Baker, and J. H. Strauss. 2002. Structure of Dengue virus: implications for Flavivirus organization, maturation, and fusion. *Cell.* 108: 717–725.

Kuikka, M., B. Ramstedt, H. Ohvo-Rekila, J. Tuuf, and J. P. Slotte. 2001. Membrane properties of D-erythro-*N*-acyl sphingomyelins and their corresponding dihydro species. *Biophys. J.* 80:2327–2337.

Kulkarni, V. S., and R. E. Brown. 1998. Thermotropic behavior of galactsylceramides with *cis*-monoenoic fatty acyl chains. *Biochim. Biophys. Acta.* 1372:347–358.

Kumar, V. V., W. H. Anderson, E. W. Thompson, B. Malewicz, and W. J. Baumann. 1988. Asymmetry of lysophosphatidylcholine/cholesterol vesicles is sensitive to cholesterol modulation. *Biochemistry.* 27:393–398.

Li, L., X. P. Tang, K. G. Taylor, D. B. Dupre, and M. C. Yappert. 2002. Conformational characterization of ceramides by nuclear magnetic resonance spectroscopy. *Biophys. J.* 82:2067–2080.

Li, X.-M., M. M. Momsen, J. M. Smaby, H. L. Brockman, and R. E. Brown. 2001. Cholesterol decreases the interfacial elasticity and detergent solubility of sphingomyelins. *Biochemistry.* 40:5954–5963.

Li, X.-M., J. M. Smaby, M. M. Momsen, H. L. Brockman, and R. E. Brown. 2000. Sphingomyelin interfacial behavior: the impact of changing acyl chain composition. *Biophys. J.* 78:1921–1931.

Lichtenberg, D., and Y. Barenholz. 1988. Liposomes: preparation, characterization, and preservation. *Methods Biochem. Anal.* 33:337–462.

Litman, B. J. 1974. Determination of molecular asymmetry in the phosphatidylethanolamine surface distribution in mixed phospholipid vesicles. *Biochemistry.* 13:2844–2848.

Malewicz, B., and W. J. Baumann. 1996. Alk-1-enylacyl, alkylacyl, and diacyl subclasses of native ethanolamine and choline glycerophospholipids can be quantitated directly by phosphorus-31 NMR in solution. *Lipids.* 31:1189–1195.

Matsuoka, K., R. Schekman, L. Orci, and J. E. Heuser. 2001. Surface structure of the COPII-coated vesicle. *Proc. Natl. Acad. Sci. USA.* 98: 13705–13709.

Mattjus, P., B. Malewicz, J. T. Valiyaveettil, W. J. Baumann, R. Bittman, and R. E. Brown. 2002. Sphingomyelin modulates the transbilayer distribution of galactosylceramide in phospholipid membranes. *J. Biol. Chem.* 277:19476–19481.

Michel, C., G. van Echten-Deckert, J. Rother, K. Sandhoff, E. Wang, and A. H. Merrill Jr. 1997. Characterization of ceramide synthesis: a dihydroceramide desaturase introduces the 4,5-trans double bond of sphingosine at the level of dihydroceramide. *J. Biol. Chem.* 272:22432–22437.

Mombelli, E., R. Morris, W. Taylor, and F. Fratermali. 2003. Hydrogen-bonding propensities of sphingomyelin in solution and in a bilayer assembly: a molecular dynamics study. *Biophys. J.* 84:1507–1517.

Niemelä, P., M. T. Hyvönen, and I. Vattulainen. 2004. Structure and dynamics of sphingomyelin bilayer: insight gained through systematic comparision to phosphatidylcholine. *Biophys. J.* 87:2976–2989.

Nordlund, J. R., C. F. Schmidt, S. N. Dicken, and T. E. Thompson. 1981. Transbilayer distribution of phosphatidylethanolamine in large and small unilamellar vesicles. *Biochemistry.* 20:3237–3241.

Nyholm, T. K. M., M. Nylund, and J. P. Slotte. 2003. A calorimeteric study of binary mixtures of dihydrosphingomyelin and sterols, sphingomyelin, or phosphatidylcholine. *Biophys. J.* 84:3138–3146.

Ohvo-Rekilä, H., P. Mattjus, and J. P. Slotte. 2002. Cholesterol interactions with phospholipids in membranes. *Prog. Lipid Res.* 41:66–97.

Pascher, I., M. Lundmark, P.-G. Nyholm, and S. Sundell. 1992. Crystal structure of membrane lipids. *Biochim. Biophys. Acta.* 113:339–373.

Ramstedt, B., P. Leppimäki, M. Axberg, and J. P. Slotte. 1999. Analysis of natural and synthetic sphingomyelins using high-performance thin-layer chromatography. *Eur. J. Biochem.* 266:997–1002.

Ramstedt, B., and J. P. Slotte. 2002. Membrane properties of sphingomyelin. *FEBS Lett.* 531:33–37.

Reed, R. A., and G. G. Shipley. 1989. Effect of chain unsaturation on the structure and thermotropic properties of galactocerebrosides. *Biophys. J.* 55:281–292.

Rietveld, A., and K. Simons. 1998. The differential miscibility of lipids as the basis for the formation of functional membrane rafts. *Biochim. Biophys. Acta.* 1376:467–479.

Ruocco, M. J., D. Atkinson, D. M. Small, R. P. Skarjune, E. Oldfield, and G. G. Shipley. 1981. X-ray diffraction and calorimetric study of anhydrous and hydrated N-palmitoylgalactosylsphingosine (cerebroside). *Biochemistry.* 20:5957–5966.

Ruocco, M. J., D. J. Siminovitch, J. R. Long, S. K. Das Gupta, and R. G. Griffin.1996. ^{2}H and ^{13}C nuclear magnetic resonance study of *N*-palmitoylgalactosylsphingosine (cerebroside)/-cholesterol bilayers. *Biophys. J.* 71:1776–1778.

Schmidt, C. F., Y. Barenholz, and T. E. Thompson. 1977. A nuclear magnetic resonance study of sphingomyelin in bilayer systems. *Biochemistry.* 16:2649–2656.

Silvius, J. R. 2003. Roles of cholesterol in lipid raft formation: lessons from lipid model systems. *Biochim. Biophys. Acta.* 1610:174–183.

Siminovitch, D. J., and K. R. Jeffery. 1981. Orientational order in the choline headgroup of sphingomyelin: a ^{14}N-NMR study. *Biochim. Biophys. Acta.* 645:270–278.

Simons, K., and E. Ikonen. 1997. Functional rafts in cell membranes. *Nature.* 387:569–572.

Simons, K., and W. L. C. Vaz. 2004. Model systems, lipid rafts, and cell membranes. *Annu. Rev. Biophys. Biomol. Struct.* 33:269–295.

Simons, M., E.-M. Krämer, C. Thiele, W. Stoffel, and J. Trotter. 2000. Assembly of myelin by association of proteolipid protein with cholesterol- and galactosylceramide-rich membrane domains. *J. Cell Biol.* 151:143–153.

Steinbauer, B., T. Mehnert, and K. Beyer. 2003. Hydration and lateral organization in phospholipid bilayers containing sphingomyelin: a ^{2}H-NMR study. *Biophys. J.* 85:1013–1024.

Stoffel, W., and A. Bosio. 1997. Myelin glycolipids and their functions. *Curr. Opin. Neurobiol.* 7:654–661.

Sweet, W. D., and F. Schroeder. 1988. Polyunsaturated fatty acids alter sterol transbilayer domains in LM fibroblast plasma membrane. *FEBS Lett.* 229:188–192.

Talbott, C. M., I. Vorobyov, D. Borchman, K. G. Taylor, D. B. DuPre, and M. C. Yappert. 2000. Conformational studies of sphingolipids by NMR spectroscopy. II. Sphingomyelin. *Biochim. Biophys. Acta.* 1467:326–337.

Théry, C., L. Zitvogel, and S. Amigorena. 2002. Exosomes: composition, biogenesis, and function. *Nat. Rev. Immunol..* 2:569–579.

van Meer, G., and Q. Lisman. 2002. Sphingolipid transport: rafts and translocators. *J. Biol. Chem.* 277:25855–25858.

Victorov, A. V., N. A. Jane, T. F. Taraschi, and J. B. Hoek. 1997. Packing constraints and electrostatic surface potentials determine transmembrane asymmetry of phosphatidylethanol. *Biophys. J.* 72:2588–2598.

Victorov, A. V., T. F. Taraschi, and J. B. Hoek. 1996. Phosphatidylethanol as a ^{13}C-NMR probe for reporting packing constraints in phospholipid membranes. *Biochim. Biophys. Acta.* 1283:151–162.

Vorobyov, I., M. C. Yappert, and D. B. Dupre. 2002. Energetic and topological analyses of cooperative sigma H- and pi H-bonding interactions. *J. Phys. Chem.* 106:10691–10699.

Warschawski, D. E., P. Fellmann, and P. F. Devaux. 1996. High-resolution ^{31}P-^{1}H two-dimensional nuclear magnetic resonance spectra of unsonicated lipid mixtures spinning at the magic-angle. *Eur. Biophys. J.* 25: 131–137.

Williams, E. E., J. A. Cooper, W. Stillwell, and L. J. Jenski. 2000. The curvature and cholesterol content of phospholipid bilayers alter the transbilayer distribution of specific molecular species of phosphatidylethanolamine. *Mol. Membr. Biol.* 17:157–164.

Wolfers, J., A. Lozier, G. Raposo, A. Regnault, C. Théry, C. Masurier, C. Flament, S. Pouzieux, F. Faure, T. Tursz, E. Angevin, S. Amigorena, and others. 2001. Tumor-derived exosomes are a source of shared tumor rejection antigens for CTL cross-priming. *Nat. Med.* 7:297–303.

Yappert, M. C., and D. Borchman. 2004. Sphingolipids in human lens membranes: an update on their composition and possible biological implications. *Chem. Phys. Lipids.* 129:1–20.